

Long-Term Stability of a Combined Cycle Plant and Two Interconnected Oil Platforms

S. Henschel

Siemens AG, EV SE NC
Paul-Gossen-Str. 100
90515 Erlangen, Germany

V. Rygg

Siemens AS, Oil & Gas
Østre Aker vei 90
0518 Oslo, Norway

T. Lauvdal

Norsk Hydro Production AS
Postboks 7190
5020 Bergen, Norway

Abstract – This paper presents an analysis of the electrical stability of two North Sea oil platforms, Snorre TLP and Snorre B, which are to be interconnected by a subsea cable of 10.5 km length. While the older platform TLP is equipped with a standard configuration of three gas turbines (one standby), the new platform B houses a combined cycle plant consisting of two gas turbines and an intermediate pressure steam turbine. The modelling of the combined cycle plant and its control and protection strategies are presented. Simulation results show the impact of the controls on the rotary stability and long-term dynamics of the platform systems.

Keywords: Industrial application, combined cycle generation, long-term stability, active power and frequency control, power system modelling.

I. INTRODUCTION

Combined cycle plants (CCP) appear to combine many advantages for practical platform operation, both with respect to economical considerations such as power capacity versus generator weight and size, and with regards to compliance with increasingly tougher environmental regulations. This gives reason to believe that CCP's will become the preferred type of platform generation in the next few decades. Parallel to this development, there has been a recent trend toward installing subsea interconnections between various platforms. This allows power sharing among platforms to improve the loading of the gas turbines, whose efficiency is much reduced when operating at low load levels.

In this light, Siemens and Norsk Hydro have conducted an extensive analysis of the feasibility and stability of the interconnected platforms, Snorre TLP (i.e. Tension Leg Platform) and Snorre B off the Norwegian shore.

A schematic diagram of the platforms is shown in Fig. 1. The Snorre B platform houses the CCP which consists of two gas turbines and one steam turbine. Snorre TLP is equipped with a standard configuration of three gas turbine generators, one of which is standby. The overall power demand on Snorre TLP is approx. 62.5 MVA, whereas 56 MVA are needed on Snorre B.

Even with all three generators in service, the foreseen load demand on Snorre TLP is likely to exceed the available power reserve in the years to come. In order to provide the lacking power for this platform, a 10.5 km subsea cable connection to Snorre B is presently planned.

The presented long-term dynamics study was initiated lest a particular loading scenario or electrical contingency could lead to such a significant drop of thermal energy and steam pressure that would necessitate a shut-down of the CCP. A complete black-out of the Snorre B platform would be the worst-case consequence.

For this analysis and other investigated aspects, a very detailed model of both platforms and the subsea connection has been built. While it would be beyond the scope of this paper to present all the modelling details for this analysis, the main aspects concerning the modelling for long-term simulation are described in Sections II–IV. These sections include a simplified representation of the CCP, and a description of the control and protection philosophies. Note that the modelling detail is not suited for electromagnetic transients simulation or harmonics analysis. The simulation results of a worst-case contingency are presented and discussed in Section V. Section VI concludes the paper.

II. COMBINED CYCLE PLANT

The combined cycle plant consists of two gas turbines (GTA, GTB) and one steam turbine (ST). The data of the respective generators is given in Table I. A model of the gas turbines is presented in Fig. 2. Besides the gas turbine, details of the speed governor and temperature control are shown. The elements reflecting the behavior of the fuel gas temperature and of the exhaust flow have been represented in great detail as they determine the interaction with the steam turbine during combined cycle operation. Owing to the complexity of the model, some characteristic relationships have been condensed in the blocks F1, F2, and F3. These functions are described below.

While an accurate model of the combined cycle plant would require intense application of thermodynamics and combustion theory [1],[2], these processes can generally be simplified to a degree suitable for the purpose of system dynamics analysis [3],[4].

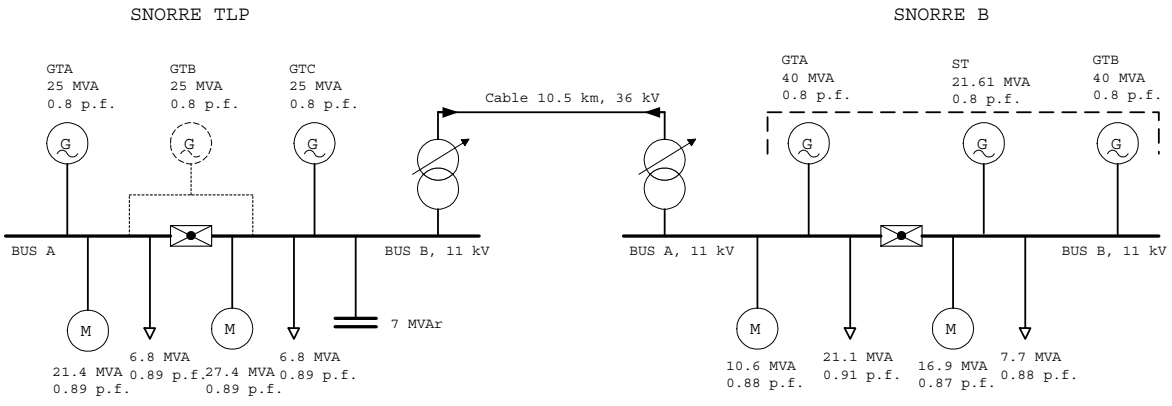


Fig. 1. Interconnected platforms Snorre TLP and B

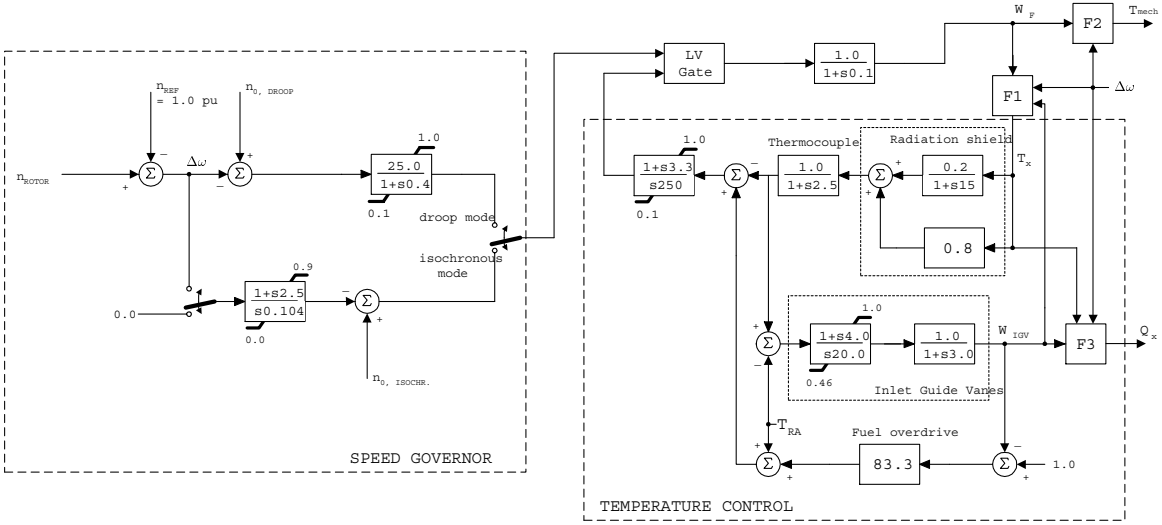


Fig. 2. Gas turbine model

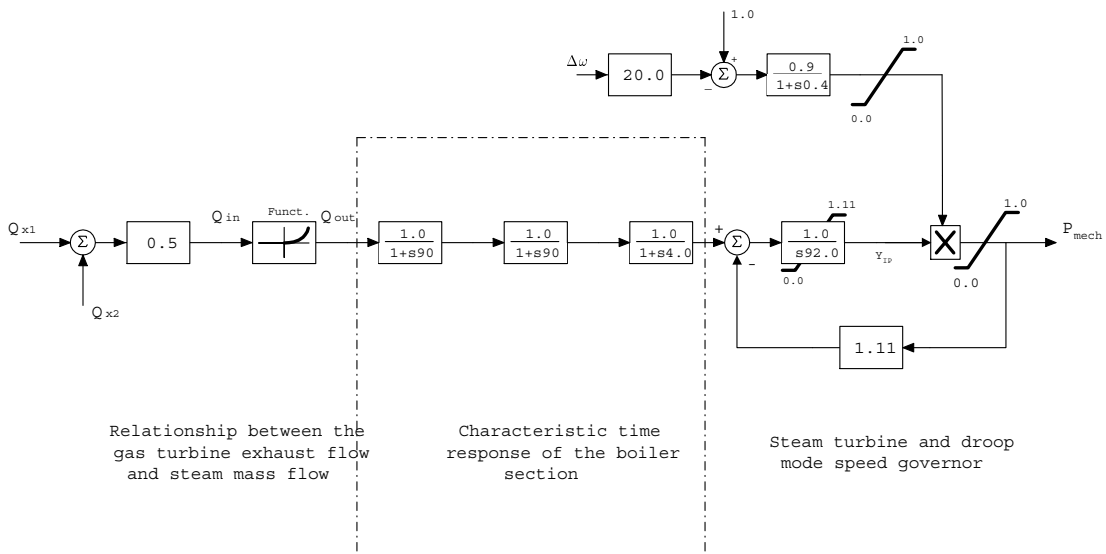


Fig. 3. Boiler and steam turbine models

TABLE I
SNORRE B: GENERATOR DATA

		GTA GTB	ST
MVA-rating	MVA	40.0	21.61
rated voltage	kV	11.0	11.0
power factor	–	0.8	0.8
frequency	Hz	60.0	60.0
T_M (starting time)	s	4.0	6.0
T_a (aperiodic time)	s	0.140	0.120
X_ℓ	pu	0.140	0.120
X_d	pu	1.690	1.880
X'_d (saturated)	pu	0.233	0.285
X''_d (saturated)	pu	0.149	0.162
X_q	pu	1.580	1.790
X'_q (saturated)	pu	0.306	0.850
X''_q (saturated)	pu	0.147	0.160
T'_d (short-circuit)	s	0.840	0.850
T''_d (short-circuit)	s	0.022	0.024
T'_q (short-circuit)	s	0.188	0.188
T''_q (short-circuit)	s	0.022	0.022

A. Calculation of the Exhaust Temperature

The turbine exhaust temperature is usually affected by many influences. The main influences however can be characterized as the fuel gas mass flow, W_F , rotor speed variations, $\Delta\omega$, and the position of the inlet guide vane, W_{IGV} , which can vary between 0.46 pu and 1 pu. This corresponds to a vane tilting angle between 57 and 84 degrees, respectively. All these influences act on a constant temperature control reference point, T_{RA} , for constant firing temperature. Mathematically, this is expressed as follows:

$$F1 = T_{RA} - 390(1 - W_F) - 306\Delta\omega + 163(1 - W_{IGV}) \quad (1)$$

The temperature control reference value depends primarily on the compressor discharge pressure, which has been assumed to be constant in this model. The control point then becomes a linear function of ambient temperature T_A :

$$T_{RA} = T_R - 0.6(T_{ISO} - T_A), \quad (2)$$

where $T_R = 541^\circ\text{C}$ is the rated exhaust temperature. Note that (1) becomes inaccurate if the ambient temperature differs considerably from ISO conditions. For simplicity, we have assumed ISO temperature, that is $T_A = T_{ISO} = 15^\circ\text{C}$.

B. Calculation of the Turbine Torque

The mechanical torque that is exerted on the rotor shaft by one of the gas turbines is described as

$$F2 = \frac{1}{0.9} (W_F - 0.1) - 5 \times 10^{-4} \omega \quad (3)$$

A minimum fuel gas flow of $W_{F,min} = 0.1$ pu is required to unlock the rotor shaft. Furthermore, there

is a small speed-dependent influence to represent rotor friction in the bearings. Normally this factor can be neglected, however, in long-term studies, it determines the slowing rate of the rotor when turbine firing is stopped.

C. Calculation of the Exhaust Flow

For the combined cycle operation, the mass flow of the exhaust gases determines the amount of thermal energy that can be absorbed by the steam in the boiler section. The following formula gives an approximation for the exhaust gas mass flow, W_x :

$$W_x = (1 + \Delta\omega) \times W_{IGV}^{0.257} \times \frac{288}{273 + T_A} \quad (4)$$

With $T_A = 15^\circ\text{C}$, the last factor becomes 1.0 and can be dropped from the equation. The thermal power, Q_x , that can be used for combined cycle operation is proportional to the mass flow times the temperature difference between exhaust temperature, $T_x = F1$, and the temperature, T_{exit} , with which the exhaust gas leaves the machine. In per units:

$$F3 = Q_x = W_x \frac{T_x - T_{exit}}{T_{RA} - T_{exit}} \quad (5)$$

The exiting temperature of the exhaust gas was assumed to be 98°C .

D. Boiler Section and Steam Turbine

A block diagram of the steam turbine model used in this study is presented in Fig. 3. In the heat exchanger, the exhaust power of both gas turbines is related to the generated thermal energy to produce steam power. This relationship in per unit is given by:

$$Q_{out} = \frac{1}{0.9^2} (Q_{in} - 0.1) \quad (6)$$

where Q_{in} is the addition of both gas turbines' exhaust powers, Q_x , and division by 2 in order to obtain per unit values.

The steam chest and boiler section are represented by a series of characteristic time delays which establish the relationship between the heating power in (6) and the steam mass flow [5]. The associated time constants are in the order of several minutes. Note that there is only a medium pressure (18 bar) section in this application; the model could be easily expanded to represent a high pressure section and reheat duct, however.

The resulting steam mass flow is led directly into the turbine where it is expanded to produce a mechanical torque on the rotor shaft. The steam is then led through the condenser and pumped back to the economizer. The steam valve is controlled by a droop mode governor shown in Fig. 3.

TABLE II
SNORRE B: 11 kV MOTOR DATA

		1	2	3	4	5	6	7
switchboard bus	–	A	B	B	B	B	A	B
mechanical power	kW	5480	5480	1360	1360	5900	4300	1250
efficiency η	%	96.0	96.0	96.4	96.4	97.4	97.3	96.3
rated $\cos \phi_n$	–	0.87	0.87	0.86	0.86	0.86	0.89	0.86
rated slip s_n	%	1.19	1.19	0.474	0.474	0.367	0.562	0.449
breakdown torque T_p	pu	1.98	1.98	2.41	2.41	2.00	2.00	2.58
starting torque T_a	pu	0.48	0.48	0.69	0.69	0.45	0.52	0.86
starting current I_a	pu	4.5	4.5	6.4	6.4	5.5	5.4	6.3
starting $\cos \phi_a$	–	0.26	0.26	0.32	0.32	0.21	0.23	0.33
shaft inertia J	kgm ²	185	185	35.8	35.8	495	465	15.2
normal loading P	pu	0.91	0.91	1.0	1.0	0.93	0.93	0.80

III. PLATFORM LOADS

Fig. 1 shows the equivalent loads and high-voltage induction motors, which comprise pipeline compressors, seawater lift pumps and water injection pumps. Besides the feeders to the low-voltage drilling stations, emergency switchboard and living quarter distribution networks, there are 19 high-voltage motors connected to the main switchboard on Snorre TLP, while there are 7 high-voltage motors on Snorre B. The data of the latter is shown in Table II. All high-voltage motors and some of the low-voltage motors are represented as detailed dynamic models, obtained from provided torque characteristics by parameter identification. Owing to their fast dynamic response, AC motor drives and other low-voltage loads are modelled by passive elements (Thevenin equivalent circuit).

IV. SYSTEM CONTROL & PROTECTION

The general operating mode of the speed controls for the gas turbines on Snorre B and TLP is isochronous mode. While droop mode had been assumed in a prior study, Fig. 4 reveals an important difference for long-term analysis: In droop mode there would be a post-fault frequency deviation from 60 Hz which would last indefinitely if it is not corrected by additional secondary, i.e. slower acting, frequency controls. In isochronous mode however, the frequency quickly returns to 60 Hz, assuming that the respective gas turbine has sufficient power reserves to establish a balance between generated and consumed power at that frequency. The steam turbine of the combined cycle system on Snorre B is not intended to fulfill primary control actions such as speed regulation. Its power generation is therefore governed by a 4 % speed droop.

In order to avoid the hunting phenomenon [6] caused by isochronously controlled gas turbines on the platforms, a load-sharing system is in place to establish equal power supply from all gas turbine generators. In addition, there is an automatic power transfer and load (APTL) control system which acts on the gas turbines on Snorre B to establish a defined power transfer of 22 MW to Snorre TLP. With this defined power transfer,

inter-platform hunting can be avoided. While the dynamics involved with power transfer controls are usually slow, i.e. order of several seconds, the response time of the APTL is in the range of a few hundred milliseconds to prevent hunting. This device therefore plays an integral part not only in long-term analysis but also in transient stability investigations.

The reactive power transfer between the platforms is minimized through tap changer controls at the transformers to the 36 kV subsea cable. To provide additional reactive power on Snorre TLP, a capacitor bank is installed. This way, the voltage drop during start-up of large induction motors can be contained to an acceptable level. Primary voltage control is left to the excitation systems of the generators. They have been modelled with standard IEEE Type 2 exciters.

With regards to the protection system, there is a load-shedding system superimposed to regular induction motor protection. This shedding system has been devised for intentional fast-tripping of certain motor loads in fault situations in order to prevent turbines and generators from overloading.

In order to determine the number of loads to be shed, the system constantly calculates and compares the amounts of available power generation and of consumed power. A drop in available power generation, e.g. by tripping a generator due to an internal failure, would then cause an equal amount of load to be shed.

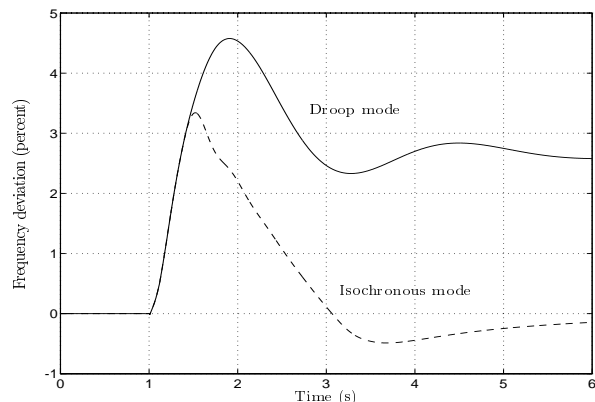


Fig. 4. Comparison of droop mode and isochronous mode governors for GTB on Snorre B

It is quite obvious that even in such relatively small power system, there is a vast number of possible switch configurations so that calculating these amounts is not a trivial task. A simplified shedding system has therefore been modelled which only monitors the circuit-breaker positions essential for the analysed cases.

V. SIMULATION RESULTS

The simulated case that is presented here assumes a worst-case situation, in which a simultaneous three phase fault occurs at Bus A of Snorre B's 11 kV main switchboard. Because of the high short-circuit current, it can be expected that the Ip-limiter trips and separates Buses A and B in, at the most, 5 ms.

The busbar protection isolates the fault in 115 ms by tripping the generator GTA, the cable connection to Snorre TLP and all outgoing feeders. As a result of the changed system configuration, the protective load-shedding system determines a power imbalance and executes its predefined shedding sequence: the high-voltage water injection pump no. 2 (see Table II) on Snorre B and 29 MVA of motor loads on Snorre TLP are tripped 110 ms and 170 ms, respectively, after the Is-limiter trip.

A. Transient Stability Analysis

Due to the fast separation of Buses A and B, the initial rotor dynamics of the generators, ST and GTB, are hardly affected by the fault itself. The temporary acceleration that can be noticed in Fig. 5 is primarily due to the changed load situation at Bus B. The sudden unloading of these generators is aggravated by tripping water injection pump no. 2. In order to bring the speed back to normal, the isochronous governor of GTB minimizes the power output of that turbine. The steam turbine also reduces its power generation yet, as the rotors speeds return to 3600 rpm, it resumes its pre-fault operating point.

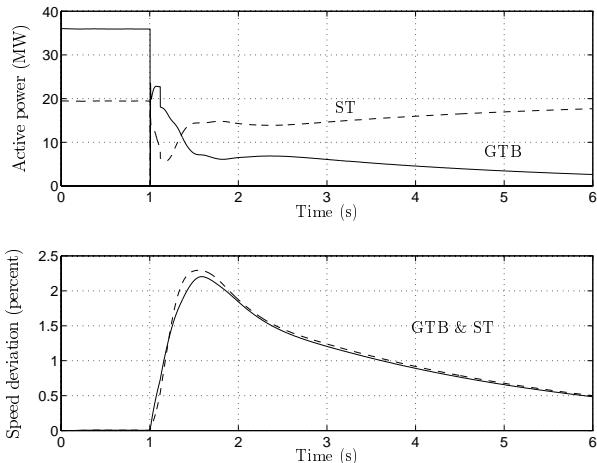


Fig. 5. Post-fault behavior at Snorre B

This causes the gas turbine GTB to further reduce its power output in order to maintain the power balance at synchronous speed. These processes occur in the first 5 seconds after the fault as shown in Fig. 5. Note that, at the moment of separation of the Buses A and B, the load-sharing system for GTA and GTB becomes ineffective.

The situation is different for the generators on Snorre TLP. Here, the fault and subsequent tripping of the cable connection mean a loss of 22 MW of power from Snorre B. This leads to a temporary overloading of the two gas turbines GTA and GTC, as shown in Fig. 6. This is accompanied by a sudden deceleration of the rotors. Since the gas turbines were at their maximum loading level prior to the fault, their temperature controls take the lead over speed control (see Fig. 2).

A continued deceleration of the rotors would be the consequence. This is prevented by the load-shedding 175 ms after the fault. This way an approximate power balance is established, and the rotor speed increases again. Note that the gas turbines remain in temperature control mode for several seconds, while the frequency stabilizes little above system frequency.

As can be seen, there is no danger of rotary instability, with fault durations of 115 ms. In fact, the interconnected platform system is stable with respect to rotor oscillations for much longer fault durations. What seems to be more problematic is that the sudden voltage drop during the fault leads to a general slow-down of the induction motor loads. After fault clearing, these motors draw a large amount of reactive starting power to re-accelerate to their normal speeds. This causes quite a significant sag of the post-fault voltage (not shown in this paper). Fault durations longer than 185 ms cause such low voltage levels during re-acceleration of the motors that some large pumps cannot be brought back to normal operation and must be shut down.

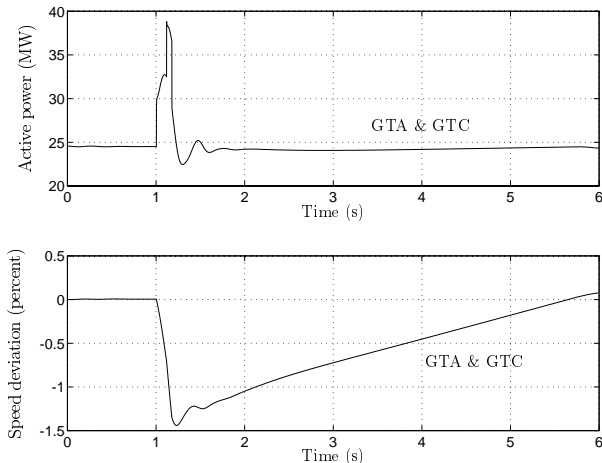


Fig. 6. Post-fault behavior at Snorre TLP

Fig. 7 shows the power output of the generators GTB and ST on Snorre B over a period of 10 minutes. Also shown is the thermal energy stored in the boiler section of the combined cycle plant. It can be seen that the power drop of GTB due to its isochronous speed control and the shut-down of GTA after the fault lessen the amount of thermal energy, since the unloaded machines do not produce an adequate level of heat.

Consequently, the steam turbine cannot longer maintain this level of power generation and reduces its output. However, the feared black-out due to overloading does not occur because the isochronous gas turbine control senses the slight drop of frequency and corrects the situation by injecting more power. This way, the power generation is smoothly transferred from the steam turbine, ST, to the gas turbine, GTB, until a stable operating point is achieved for both turbines.

C. Simulation Aspects

The simulations have been performed with the power system simulation tool NETOMAC[®] by Siemens. After the fault scenario and the decay of fast rotor transients, the simulation time step is increased from 3 ms to 300 ms for long-term simulation.

Unlike in programs such as ETMSP [7], the simulation time step is here simultaneously applied to all models. Considerations of the stiffness of the differential equations show that the response time of all used models are sufficiently long to permit this choice of time steps.

While transient network dynamics, i.e. electromagnetic transients, are typically too fast for an accurate simulation with these time steps [8], their impact on the machine and boiler dynamics is approximated by the quasi-steady state admittance matrix representation of the electric network. This is common practice in stability analysis, and its implications have been well documented, e.g. in [6].

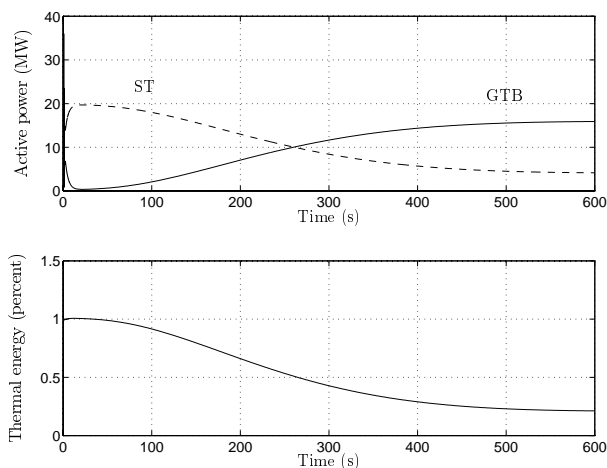


Fig. 7. Long-term behavior of Snorre B

This paper has demonstrated several important aspects that should be considered for combined cycle generation on interconnected oil platform systems. For a rigid analysis of the electrical stability of such systems, both transient rotor dynamics and long-term boiler dynamics must be investigated.

While an accurate simulation of the rotor dynamics requires detailed models of the platform machines, mid-term and long-term dynamics are primarily influenced by the turbine controls and boiler characteristics. This article illustrates these aspects with a model of the Norwegian interconnected platforms, Snorre TLP and B. Detailed models of the gas and steam turbines of the combined cycle plant on Snorre B and their associated controls have been presented. Practical strategies for system control and protection have been discussed.

The simulation results have shown that it is highly improbable that the combined cycle steam turbine would run out of steam due to an electrical contingency or unforeseen loading condition, and cause a black-out of the entire platform. As long as the gas turbine GTB has a sufficient amount of power reserves, its isochronous speed governor will prevent an overloading of the steam turbine and establish a stable post-fault operating point for both turbines.

References

- [1] H. A. van Essen, *Modelling and Model Based Control of Turbomachinery*, Ph.D. Thesis, Cip-Data Library Technische Universiteit Eindhoven, Netherlands, 1998, ISBN 90-386-0830-6.
- [2] A. H. Lefebvre, *Gas Turbine Combustion*, McGraw-Hill Series in Energy, Combustion and Environment, Hemisphere Publishing Corporation, New York, NY, U.S.A., 1983, ISBN 0-07-037029-X.
- [3] B. Schönfeld, *Modellbildung eines Kombi-Kraftwerks zur Untersuchung des Systemverhaltens mit dem Netz (Combined Cycle Plant Modelling for the Analysis of Power System Interaction)*, Ph.D. Thesis, Technical University of Berlin, Verlag Shaker, Aachen, Germany, 1993, ISBN 3-86111-635-9.
- [4] F. P. de Mello, "Boiler Models for System Dynamic Performance Studies," *IEEE Transactions on Power Systems*, vol. 6, pp. 66-74, February 1991.
- [5] VDI/VDE, "Blockregelung von Wärmekraftwerken. (Control of Thermal Power Units)," *VDI/VDE-Guidelines*, no. 3508, July 1984.
- [6] P. Kundur, *Power System Stability and Control*, EPRI Power System Engineering Series. McGraw-Hill, Inc., New York, NY 10020, U.S.A., 1994, ISBN 0-07-035958-X.
- [7] E. G. Cate, K. Hemmaplardh, J. W. Manke and D. P. Gelopoulos, "Time Frame Notion and Time Response of the Models in Transient, Mid-Term and Long-Term Stability Programs," *IEEE Transactions on Power Apparatus and Systems*, vol. 103, no. 1, pp. 143-151, January 1984.
- [8] H. W. Dommel, *EMTP Theory Book*, Microtran Power System Analysis Corporation, 4689 W. 12th Avenue, Vancouver, B.C. V6R 2R7, Canada, 2nd edition, May 1992.